EUROPEAN ORGANIZATION FOR NUCLEAR RESEARCH

CERN-PPE/91-114
16 July 1991

Production and Decay of Charmed Mesons at the Z Resonance

The ALEPH Collaboration*

Abstract

In a sample of 190,000 hadronic Z decays, three signals of charm production are observed: two from the exclusive decays $D^0 \to K^-\pi^+$ and $D^{*+} \to D^0\pi^+ \to K^-\pi^+\pi^+$ and one in the transverse-momentum distribution of soft hadrons relative to the nearest jet. The features of these signals are in good agreement with expectations based on the Standard Model and previous measurements of the branching fractions. The number of $D^{*\pm} \to K^\mp\pi^\pm\pi^\pm$ per hadronic decay of the Z is measured to be $(5.11 \pm 0.34) \times 10^{-3}$, and the branching ratio $B(D^0 \to K^-\pi^+)$ is $(3.62 \pm 0.34 \pm 0.44)\%$. Charm hadronization has been studied. The average fraction of the beam energy carried by the D^* meson is found to be $\langle X_E \rangle_c = 0.504 {}^{+0.013}_{-0.017} \pm 0.008$, and implications of the measurements on the pseudoscalar-to-vector production ratio of charmed mesons are discussed.

(Submitted to Physics Letters B)

*See the following pages for the list of authors.

The ALEPH Collaboration

D. Decamp, B. Deschizeaux, C. Goy, J.-P. Lees, M.-N. Minard

Laboratoire de Physique des Particules (LAPP), IN^{2}P^3-CNRS, 74019 Annecy-le-Vieux Cedex, France

R. Alemany, J.M. Crespo, M. Delfino, E. Fernandez, V. Gaitan, Ll. Garrido, Ll.M. Mir, A. Pacheco

Laboratorio de Fisica de Altas Energias, Universidad Autonoma de Barcelona, 08193 Bellaterra (Barcelona), Spain[8]

M.G. Catanesi, D. Creanza, M. de Palma, A. Farilla, G. Iaselli,[1] G. Maggi, M. Maggi, S. Natali, S. Nuzzo, M. Quattromini, A. Ranieri, G. Raso, F. Romano, F. Ruggieri, G. Selvaggi, L. Silvestris, P. Tempesta, G. Zito

INFN Sezione di Bari e Dipartimento di Fisica dell' Università, 70126 Bari, Italy

Y. Gao, H. Hu,[21] D. Huang, X. Huang, J. Lin, J. Lou, C. Qiao,[21] T. Ruan,[21] T. Wang, Y. Xie, D. Xu, R. Xu, J. Zhang, W. Zhao

Institute of High-Energy Physics, Academia Sinica, Beijing, The People's Republic of China[9]

W.B. Atwood,[2] L.A.T. Bauerdick, F. Bird, E. Blucher, G. Bonvicini, F. Bossi, J. Boudreau, D. Brown, T.H. Burnett,[3] H. Drevermann, R.W. Forty, C. Grab, R. Hagelberg, S. Haywood, J. Hilgart, B. Jost, M. Kasemann, J. Knobloch, A. Lacourt, E. Lançon, I. Lehraus, T. Lohse, A. Lusiani, A. Marchioro, M. Martinez, P. Mato, S. Menary, A. Minten, A. Miotto, R. Miquel, H.-G. Moser, J. Nash, P. Palazzi, F. Ranjard, G. Redlinger, A. Roth, J. Rothberg,[3] H. Rotscheidt, M. Saich, R. St.Denis, D. Schlatter, M. Takashima, M. Talby,[4] W. Tejessy, H. Wachsmuth, S. Wasserbaech, S. Wheeler, W. Wiedenmann, W. Witzeling, J. Wotschack

European Laboratory for Particle Physics (CERN), 1211 Geneva 23, Switzerland

Z. Ajaltouni, M. Bardadin-Otwinowska, R. El Fellous, A. Falvard, P. Gay, J. Harvey, P. Henrard, J. Jousset, B. Michel, J-C. Montret, D. Pallin, P. Perret, J. Proriol, F. Prulhière, G. Stimpfl

Laboratoire de Physique Corpusculaire, Université Blaise Pascal, IN^{2}P^3-CNRS, Clermont-Ferrand, 63177 Aubière, France

J.D. Hansen, J.R. Hansen, P.H. Hansen, R. Møllerud, B.S. Nilsson

Niels Bohr Institute, 2100 Copenhagen, Denmark[10]

I. Efthymiopoulos, E. Simopoulou, A. Vayaki

Nuclear Research Center Demokritos (NRCD), Athens, Greece

J. Badier, A. Blondel, G. Bonneaud, J. Bourotte, F. Braems, J.C. Brient, G. Fouque, A. Gamess, R. Guirlet, S. Orteu, A. Rosowsky, A. Rougé, M. Rumpf, R. Tanaka, H. Videau

Laboratoire de Physique Nucléaire et des Hautes Energies, Ecole Polytechnique, IN²P³-CNRS, 91128 Palaiseau Cedex, France

D.J. Candlin, E. Veitch

Department of Physics, University of Edinburgh, Edinburgh EH9 3JZ, United Kingdom[11]

L. Moneta, G. Parrini

Dipartimento di Fisica, Università di Firenze, INFN Sezione di Firenze, 50125 Firenze, Italy

M. Corden, C. Georgiopoulos, M. Ikeda, J. Lannutti, D. Levinthal,[16] M. Mermikides, L. Sawyer

Supercomputer Computations Research Institute and Dept. of Physics, Florida State University, Tallahassee, FL 32306, USA [13,14,15]

A. Antonelli, R. Baldini, G. Bencivenni, G. Bologna,[5] P. Campana, G. Capon, F. Cerutti, V. Chiarella, B. D'Ettorre-Piazzoli,[6] G. Felici, P. Laurelli, G. Mannocchi,[6] F. Murtas, G.P. Murtas, G. Nicoletti, L. Passalacqua, M. Pepe-Altarelli, P. Picchi,[5] P. Zografou

Laboratori Nazionali dell'INFN (LNF-INFN), 00044 Frascati, Italy

B. Altoon, O. Boyle, A.W. Halley, I. ten Have, J.L. Hearns, J.G. Lynch, W.T. Morton, C. Raine, J.M. Scarr, K. Smith, A.S. Thompson, R.M. Turnbull

Department of Physics and Astronomy, University of Glasgow, Glasgow G12 8QQ, United Kingdom[11]

B. Brandl, O. Braun, R. Geiges, C. Geweniger, P. Hanke, V. Hepp, E.E. Kluge, Y. Maumary, A. Putzer, B. Rensch, A. Stahl, K. Tittel, M. Wunsch

Institut für Hochenergiephysik, Universität Heidelberg, 6900 Heidelberg, Fed. Rep. of Germany[17]

A.T. Belk, R. Beuselinck, D.M. Binnie, W. Cameron, M. Cattaneo, P.J. Dornan,[1] S. Dugeay, A.M. Greene, J.F. Hassard, N.M. Lieske, S.J. Patton, D.G. Payne, M.J. Phillips, J.K. Sedgbeer, G. Taylor, I.R. Tomalin, A.G. Wright

Department of Physics, Imperial College, London SW7 2BZ, United Kingdom[11]

P. Girtler, D. Kuhn, G. Rudolph

Institut für Experimentalphysik, Universität Innsbruck, 6020 Innsbruck, Austria[19]

C.K. Bowdery,[1] T.J. Brodbeck, A.J. Finch, F. Foster, G. Hughes, N.R. Keemer, M. Nuttall, A. Patel, B.S. Rowlingson, T. Sloan, S.W. Snow, E.P. Whelan

Department of Physics, University of Lancaster, Lancaster LA1 4YB, United Kingdom[11]

T. Barczewski, K. Kleinknecht, J. Raab, B. Renk, S. Roehn, H.-G. Sander, M. Schmelling, H. Schmidt, F. Steeg, S.M. Walther, B. Wolf

Institut für Physik, Universität Mainz, 6500 Mainz, Fed. Rep. of Germany[17]

J-P. Albanese, J-J. Aubert, C. Benchouk, V. Bernard, A. Bonissent, D. Courvoisier, F. Etienne, S. Papalexiou, P. Payre, B. Pietrzyk, Z. Qian

Centre de Physique des Particules, Faculté des Sciences de Luminy, IN^{2}P^3-CNRS, 13288 Marseille, France

H. Becker, W. Blum, P. Cattaneo, G. Cowan, B. Dehning, H. Dietl, F. Dydak[26], M. Fernandez-Bosman, T. Hansl-Kozanecka,[22] A. Jahn, W. Kozanecki,[2,23] E. Lange, J. Lauber, G. Lütjens, G. Lutz, W. Männer, Y. Pan, R. Richter, J. Schröder, A.S. Schwarz, R. Settles, U. Stierlin, J. Thomas, G. Wolf

Max-Planck-Institut für Physik und Astrophysik, Werner-Heisenberg-Institut für Physik, 8000 München, Fed. Rep. of Germany[17]

V. Bertin, J. Boucrot, O. Callot, X. Chen, A. Cordier, M. Davier, G. Ganis, J.-F. Grivaz, Ph. Heusse, P. Janot, D.W. Kim,[20] F. Le Diberder, J. Lefrançois,[1] A.-M. Lutz, J.-J. Veillet, I. Videau, Z. Zhang, F. Zomer

Laboratoire de l'Accélérateur Linéaire, Université de Paris-Sud, IN^{2}P^3-CNRS, 91405 Orsay Cedex, France

D. Abbaneo, S.R. Amendolia, G. Bagliesi, G. Batignani, L. Bosisio, U. Bottigli, C. Bradaschia, M. Carpinelli, M.A. Ciocci, R. Dell'Orso, I. Ferrante, F. Fidecaro, L. Foà, E. Focardi, F. Forti, C. Gatto, A. Giassi, M.A. Giorgi, F. Ligabue, E.B. Mannelli, P.S. Marrocchesi, A. Messineo, F. Palla, G. Sanguinetti, J. Steinberger, R. Tenchini, G. Tonelli, G. Triggiani, C. Vannini, A. Venturi, P.G. Verdini, J. Walsh

Dipartimento di Fisica dell'Università, INFN Sezione di Pisa, e Scuola Normale Superiore, 56010 Pisa, Italy

J.M. Carter, M.G. Green,[1] P.V. March, T. Medcalf, I.S. Quazi, J.A. Strong, R.M. Thomas, L.R. West, T. Wildish

Department of Physics, Royal Holloway & Bedford New College, University of London, Surrey TW20 OEX, United Kingdom[11]

D.R. Botterill, R.W. Clifft, T.R. Edgecock, M. Edwards, S.M. Fisher, T.J. Jones, P.R. Norton, D.P. Salmon, J.C. Thompson

Particle Physics Dept., Rutherford Appleton Laboratory, Chilton, Didcot, Oxon OX11 OQX, United Kingdom[11]

B. Bloch-Devaux, P. Colas, C. Klopfenstein, E. Locci, S. Loucatos, E. Monnier, P. Perez, J.A. Perlas, F. Perrier, J. Rander, J.-F. Renardy, A. Roussarie, J.-P. Schuller, J. Schwindling, B. Vallage

Département de Physique des Particules Elémentaires, CEN-Saclay, 91191 Gif-sur-Yvette Cedex, France[18]

J.G. Ashman, C.N. Booth, C. Buttar, R. Carney, S. Cartwright, F. Combley, M. Dinsdale, M. Dogru, F. Hatfield, J. Martin, D. Parker, P. Reeves, L.F. Thompson

Department of Physics, University of Sheffield, Sheffield S3 7RH, United Kingdom[11]

E. Barberio, S. Brandt, H. Burkhardt,[1] C. Grupen, H. Meinhard, L. Mirabito, U. Schäfer, H. Seywerd

Fachbereich Physik, Universität Siegen, 5900 Siegen, Fed. Rep. of Germany[17]

G. Apollinari, G. Giannini, B. Gobbo, F. Liello, F. Ragusa,[25] L. Rolandi, U. Stiegler

Dipartimento di Fisica, Università di Trieste e INFN Sezione di Trieste, 34127 Trieste, Italy

L. Bellantoni, X. Chen, D. Cinabro, J.S. Conway, D.F. Cowen,[24] Z. Feng, D.P.S. Ferguson, Y.S. Gao, J. Grahl, J.L. Harton, J.E. Jacobsen, R.C. Jared,[7] R.P. Johnson, B.W. LeClaire, Y.B. Pan, J.R. Pater, Y. Saadi, V. Sharma, Z.H. Shi, Y.H. Tang, A.M. Walsh, J.A. Wear,[27] F.V. Weber, M.H. Whitney, Sau Lan Wu, G. Zobernig

Department of Physics, University of Wisconsin, Madison, WI 53706, USA[12]

---

[1]Now at CERN.
[2]Permanent adddress: SLAC, Stanford, CA 94309, USA.
[3]Permanent address: University of Washington, Seattle, WA 98195, USA.
[4]Also Centre de Physique des Particules, Faculté des Sciences, Marseille, France
[5]Also Istituto di Fisica Generale, Università di Torino, Torino, Italy.
[6]Also Istituto di Cosmo-Geofisica del C.N.R., Torino, Italy.
[7]Permanent address: LBL, Berkeley, CA 94720, USA.
[8]Supported by CAICYT, Spain.
[9]Supported by the National Science Foundation of China.
[10]Supported by the Danish Natural Science Research Council.
[11]Supported by the UK Science and Engineering Research Council.
[12]Supported by the US Department of Energy, contract DE-AC02-76ER00881.
[13]Supported by the US Department of Energy, contract DE-FG05-87ER40319.
[14]Supported by the NSF, contract PHY-8451274.
[15]Supported by the US Department of Energy, contract DE-FC0S-85ER250000.
[16]Supported by SLOAN fellowship, contract BR 2703.
[17]Supported by the Bundesministerium für Forschung und Technologie, Fed. Rep. of Germany.
[18]Supported by the Institut de Recherche Fondamentale du C.E.A..
[19]Supported by Fonds zur Förderung der wissenschaftlichen Forschung, Austria.
[20]Supported by the Korean Science and Engineering Foundation and Ministry of Education.
[21]Supported by the World Laboratory.
[22]On leave of absence from MIT, Cambridge, MA 02139, USA.
[23]Supported by Alexander von Humboldt Fellowship, Germany.
[24]Now at California Institute of Technology, Pasadena, CA 91125, USA.
[25]Now at Dipartimento di Fisica, Università di Milano, Milano, Italy.
[26]Also at CERN, PPE Division, 1211 Geneva 23, Switzerland.
[27]Now at University of California, Santa Cruz, CA 95064, USA.

1 Introduction

The study of D and D^* mesons produced at the Large Electron-Positron collider (LEP) is of special interest, as they provide a unique way of probing the c quark production at the Z resonance and its fragmentation at high energy. One expects two main sources of charmed mesons at LEP: the decay $Z \to c\bar{c}$, where a c quark hadronizes, and the decay $Z \to b\bar{b}$, where a beauty hadron subsequently decays into charm. These two sources are of comparable size. The D's and D^*'s from $b\bar{b}$ have a softer energy distribution because, even though the beauty quark has a harder fragmentation than the charm, on the average only about 1/3 of the beauty hadron momentum is transferred to the decay charmed meson. The shape of the observed energy spectrum thus depends on the relative size of the $b\bar{b}$ and $c\bar{c}$ contributions.

The very low Q value for the decay [1] $D^{*+} \to D^0\pi_s^+$ ($m_{D^*} - m_{D^0} - m_\pi = 6$ MeV/c^2) or, correspondingly, the very low momentum of the decay products in the D^{*+} rest frame ($p^* = 40$ MeV/c), places the signal in a low-background region [1]. The π^+ has its transverse momentum p_T relative to the D^* line of flight bounded by this value and takes a relatively low fraction $[O(m_\pi/m_{D^*} = 0.075)]$ of the D^* longitudinal momentum. This soft, low-p_T pion (π_s) provides an excellent signature for charm production.

Three different signals are used in this analysis:

(i) $D^0 \to K^-\pi^+$,

(ii) $D^{*+} \to D^0\pi_s^+$ exclusive decay, with subsequent $D^0 \to K^-\pi^+$,

(iii) $D^{*+} \to (D^0)\pi_s^+$ identified only by the presence of the low – momentum and low – transverse – momentum pion.

Comparison of (i) and (ii) allows an estimation of the relative production rate of vector and pseudoscalar charmed mesons; comparison of (ii) and (iii) provides a measurement of the branching ratio $D^0 \to K^-\pi^+$; and the study of the $X_E = E_{D^*}/E_{\rm beam}$ spectrum leads to a measurement of the charm fragmentation parameter.

2 ALEPH Detector and Data Selection

The ALEPH detector has been described elsewhere [2]. This analysis relies mainly on the Time Projection Chamber (TPC) and the Inner Tracking Chamber (ITC) which are situated in a 1.5 T magnetic field produced by a superconducting solenoid. A global fit to the ITC and TPC coordinates allows the track momentum to be measured with an accuracy [3, 2] of

$$\frac{\delta p}{p} = \sqrt{\left(0.0008\frac{p_T}{\mathrm{GeV}/c}\right)^2 + (0.003)^2}\ .$$

The data sample consists of 189,506 hadronic events selected by the requirement that they contain at least five charged tracks of momentum above 0.2 GeV/c and polar angle θ with the beam axis satisfying $|\cos\theta| \leq 0.95$, which implies that they cross at least six rows of cathode pads of the TPC. They must include at least 4 measured coordinates from the TPC, and their distance of closest approach to the interaction vertex must be less than 10 cm along the beam axis and less than 2 cm in the transverse plane. The sum of the momenta of all tracks meeting these conditions must be greater than 10% of the centre-of-mass energy. This selects hadronic Z decays with an

[1] Here, and in the following, charge-conjugate modes are implied.

efficiency of 97.4±0.3%, leaving a contribution of 0.7±0.1% from τ pairs and two-photon scattering [4]. The efficiency is flavour-independent except for $b\bar{b}$ events (98.0%).

Most of the data were taken at the Z peak energy; the remainder was at 1, 2, or 3 GeV above or below the peak. The use of reduced quantities (energies divided by the beam energy) allows all the data to be combined.

A Monte Carlo model including initial state radiation is used to estimate the selection efficiency, to parametrize the heavy-quark fragmentation and to give guidance on the background composition and shape. The jets are simulated according to the LUND parton shower evolution and fragmentation [5]. The light-quark fragmentation and QCD parameters were chosen to fit ALEPH data. For heavy quarks Q = b, c, the Peterson *et al.* fragmentation function [6] is used

$$f(z) = z^{-1}\left(1 - \frac{1}{z} - \frac{\varepsilon_Q}{(1-z)}\right)^{-2},$$

where z is the fraction of $(E + P_{\parallel})$ of the meson relative to the parent quark and ε_Q is a parameter giving the 'hardness' of the energy spectrum. The value of $\varepsilon_b = (6\,^{+4}_{-3})\times 10^{-3}$ has been obtained from a fit to the momentum spectrum of leptons in hadronic events [7]. The determination of ε_c is an aim of this study. The heavy-quark decays were tuned to best reproduce the latest measurements. A detailed simulation of the ALEPH detector was carried out on all the generated events. They were then subjected to the standard ALEPH reconstruction program.

3 Exclusive Decays of Charmed Mesons

A search is performed for candidates of the decays (i) with $X_E(\mathrm{D}^0) \geq 0.25$ and (ii) with $X_E(\mathrm{D}^*) \geq 0.25$. All pairs of oppositely charged tracks meeting the requirements of Section 2 are used to form both a D^0 and a $\bar{\mathrm{D}}^0$ candidate by assigning the kaon mass to one of the particles and the pion mass to the other. A combination is retained if the angle θ^*_{K} between the K and the line of flight of the Kπ system, evaluated in the Kπ centre of mass, satisfies $|\cos\theta^*_{\mathrm{K}}| \leq 0.8$. This cut is efficient in removing the combinatorial background, which peaks at $|\cos(\theta^*_{\mathrm{K}})| = 1$, while it accepts 80% of the signal, since the decay of the D^0 meson is isotropic. The Kπ mass distribution is shown in Fig. 1, where a clear enhancement in the D^0 mass region is visible. The mass range from 1.835 to 1.895 GeV/c^2 is used to define the D^0 sample.

Particle identification is not used for rejecting combinations. The fact that both mass assignments $\mathrm{K}^+\pi^-$ and $\mathrm{K}^-\pi^+$ can satisfy all the criteria leads to a certain amount of double counting. This is taken into account and was estimated by the Monte Carlo simulation to increase the signal by 20%. The background is found to contain both a 'charm' and a 'combinatorial' contribution. The 'charm' contribution is due to charmed mesons decaying – either in a resonant manner or not – into two charged particles plus others, neutral or charged. The Monte Carlo, which includes decays of the D^0, $\mathrm{D}^\pm$, and $\mathrm{D_s}$ mesons, is found to be in good agreement with the data in the low side band of the effective mass distribution. A non-negligible part of this 'charm' background spills over into the signal region owing to the widening of all these contributions by the presence of the aforementioned wrong mass assignments. The 'combinatorial' background includes all the random combinations leading to a smoothly falling mass distribution. It is fitted with a third-degree polynomial, whose shape agrees well with the Monte Carlo prediction for light quark contribution. These two contributions are also shown in Fig. 1. Subtracting the background in the signal region and correcting for double-counting leads to a signal of $1468 \pm 86(\mathrm{stat.}) \pm 83(\mathrm{syst.})$ D^0's. The systematic error comes from the background subtraction. It has been estimated by varying the fit range and the shape of the combinatorial background.

For the $D^{*\pm}$ search, one more track, the soft pion (π_s), is added. Its momentum must lie within the kinematically allowed range for a $D^{*+} \to D^0\pi_s^+$ decay with $0.25 \leq X_E(D^*) \leq 1$, i.e. 0.55 to 4.2 GeV/$c$. Here the mass assignment is unambiguous, as the charge of the K must be opposite to that of the soft pion. All the cuts are the same as for process (i), except that here X_E refers to the D^* instead of the D^0. The distribution of the mass difference $\Delta M = M(K\pi\pi_s) - M(K\pi)$ shows evidence for D^* production (Fig. 2). The $K\pi$ invariant mass distribution for the combinations which satisfy $0.1435 \leq \Delta M \leq 0.1475$ GeV/c^2, shown in Fig. 3, exhibits a clear D^0 signal from $D^{*\pm}$ decays. The number of combinations selected by these two simultaneous mass cuts is 431.

Fits to these mass distributions have been performed using the shape of the signals as predicted by the Monte Carlo and leaving the mass difference and the D^0 mass as free parameters. The best fits are obtained for $\Delta M = 145.30 \pm 0.06$ and $m_{D^0} = 1863.5 \pm 0.9$ MeV/c^2, where the quoted errors are statistical only. These are consistent with previous measurements [8, 9] and [10], respectively. Fits with analytic functions have also been carried out using a simple form for the background and the sum of two Gaussians for the signal (Fig. 2a). The half widths at half maximum are respectively 0.8 MeV/c^2 for ΔM and 18 MeV/c^2 for the two-body mass, in good agreement with the Monte Carlo simulation.

To estimate the background size and its X_E dependence, an event mixing technique is used. The pions are taken from one event and the kaon is taken from another. The jet containing the kaon is then rotated so as to make its axis coincide with that of the jet of the pions. This procedure has the advantage over the Monte Carlo of being practically not limited by statistics, as one event can be mixed with many others. The number of background events within the cuts is estimated from the mass-difference spectrum. The shape of the background is taken from the event mixing and normalized to the data in the upper side band defined by $\Delta M \geq 0.152$ GeV/c^2. Its integral in the peak region is then taken as the number of expected background combinations. This gives a value of 77±3 background events. The same method has been applied to the $K\pi$ mass spectrum and gives 81±6 background events. The quoted uncertainty comes from the statistical fluctuations on the background normalization. From the spread between the various fits, the systematic uncertainty on the expected number of background events is estimated to be ±5.

The shape of the background X_E spectrum obtained from event mixing has been compared with that obtained from the upper side bands of the two distributions of Figs. 2 and 3 and was found to be in good agreement. It is also consistent with the result of the more direct – though statistically more limited – method of subtracting the background in the ΔM distribution bin by bin in X_E. The background is much steeper than the signal, which justifies the cut at X_E=0.25.

The selection efficiency has been evaluated with the Monte Carlo, and cross-checked for each cut with the data. It depends on X_E, ranging from 55% at X_E=0.25 down to 40% at X_E=1. This decrease is due to the widening of the two-body mass distribution with increasing D^0 momentum. The detection and selection efficiency can be broken up into four main contributions: 90% for the angular and momentum cuts on tracks and for losses at low angle, 80% for the $|\cos\theta_K^*| \leq 0.8$ cut, 90% for the ΔM cut, and 80% for the two-body mass cut. The systematic error on track-reconstruction efficiency has been estimated by scanning over 5000 tracks. The difference between the real and Monte Carlo track-reconstruction efficiency has been found to be negligible within our angular and momentum cuts. The uncertainty on the efficiency of the mass cuts has been evaluated by using the parametrization fitted to the data and varying the width and average between two extreme values compatible within $\pm 1\sigma$ with the data. As a result, the global relative error on the efficiency is $\delta\epsilon/\epsilon = \pm 0.036$, of which ±0.025 comes from each of the two mass cuts.

4 Measurement of (D^0 from D^{*+})/(all D^0)

The ratio R_* of the number of D^0's from D^{*+} decays to the total number of D^0's can be used to estimate the probability P_V of producing a charmed vector meson rather than a pseudoscalar: $P_V = V/(V+P)$ (notation of Ref. [11]). Indeed, a D^0 can either be directly produced or be the decay product of a $D^{*\pm}$ (with a branching fraction $B_* = 55 \pm 4\%$ [10]) or of a D^{*0} (100% branching fraction). Assuming that, among the direct D and D* mesons, the number of charged and neutrals are equal, the ratio R_* can be written as

$$R_* = \frac{P_V B_*}{P_V B_* + 1} .$$

The measurement of R_* proceeds as follows. For the number of D^0's from $D^{*\pm}$, the same analysis as for the $D^{*\pm}$ search is performed, except that the X_E cut is applied to the D^0 rather than the parent D^*. The resulting number of events, corrected for the ΔM cut, is 363±22. The systematic uncertainty on the relative efficiency between the numerator and the denominator is limited to ±2.5% from the ΔM cut, as the selection is the same in both cases. The result is $R_* = 0.247 \pm 0.020 \pm 0.013$, which leads to $P_V B_* = 0.329 \pm 0.040$. Using the above value for B_*, we obtain $P_V = 0.60 \pm 0.08 \pm 0.05$, where the first error is internal to this analysis and the second comes from the branching ratio B_*.

Since this result is obtained from a mixture of $b\bar{b}$ and $c\bar{c}$ events, the interpretation of P_V in terms of charm hadronization is not straightforward. The hadronic environment is different for charm quarks that are directly produced in Z decays as opposed to those produced in decays of beauty hadrons. Therefore the same analysis has been repeated in two X_E ranges: for the $b\bar{b}$-dominated region, $X_E \le 0.5$ (b purity = 65%), $P_V = 0.58 \pm 0.12 \pm 0.05$ is found, and for the $c\bar{c}$-dominated region, $X_E \ge 0.5$ (c purity = 76%), $P_V = 0.65 \pm 0.12 \pm 0.05$. The latter result is consistent with the CLEO result [11] ($0.80 \pm 0.12 \pm 0.06$), derived from their measurement of $P_V B_*$ by the procedure described here, with a nearly pure $c\bar{c}$ sample[2].

The competing production of higher mass states [13], hereafter called D**'s, can affect this measurement. Assuming that a fraction H of the c quarks hadronizes into D**, and letting B_{**} be the average branching fraction $B(D^{**} \to D^{*\pm}X)$, the above relation becomes

$$R_* = \frac{Y}{Y+1} ,$$

where

$$Y = P_V B_* + H(2B_{**} - P_V)B_* .$$

It is assumed that equal numbers of charged and neutral mesons are produced. Taking H to be around 15%, and allowing for the largest possible range (0 to 0.5) for B_{**}, P_V could differ by as much as ±20% from the above value. Larger statistics and additional observations, including the D**, are needed to obtain a more conclusive measurement of the vector-to-pseudoscalar ratio from the ratio R_*.

5 Charm Fragmentation and $D^{*\pm}$ Production Rate

Fitting the X_E distribution allows a measurement of the fragmentation parameter ε_c. The observed X_E distribution includes contributions from three sources: D*'s from $c\bar{c}$, D*'s from $b\bar{b}$, and

[2]Notice that if the new and preliminary CLEO2 measurement of $B_* = (67.8 \pm 3.2 \pm 1.5)\%$ [12] is confirmed, all the P_V values given here will be lowered by 20%.

background from all flavours. There are five parameters: the size of each contribution, and the shape parameters ε_c and ε_b. The ALEPH measurement of ε_b from semileptonic b-decay studies [7] is already accurate enough that its variation within errors does not significantly affect the fit. The shape and normalization of the background contribution are obtained from the study described in Section 3. However, the relative contribution of $b\bar{b}$ and $c\bar{c}$ cannot be fitted with any reasonable statistical accuracy. One additional piece of information is therefore needed to allow the fit to converge. The choice which is retained in the following is to fix the ratio of the number of $D^{*\pm}$ per primary b quark to the number of $D^{*\pm}$ per primary c quark

$$(b/c) \equiv \frac{P_{b\to D^{*\pm}}}{P_{c\to D^{*\pm}}} .$$

Measurements of this ratio give results consistent with unity, but with large uncertainties, and have been carried out at lower energies, where B_s and beauty baryons are not produced. We prefer to use the value $(b/c) = 0.95$ calculated from our Monte Carlo model, which contains estimates of the branching fractions from measurements, symmetry arguments, and simple modelling of the unknown decays. This introduces a model dependence of the results, which will be quantified by letting (b/c) vary between 0.85 and 1.05.

A binned log-likelihood fit to the $X_E(D^*)$ distribution is performed with the function

$$\frac{dN}{dX_E} = N_{had} \times 2 \times P_{c\to D^{*\pm}}\, B_*\, B_0\, \epsilon(X_E)\, f_{HF}(X_E,\varepsilon_c) \;+\; f_{BG}(X_E) .$$

N_{had} is the number of hadronic events corrected for $\tau^+\tau^-$ and $\gamma\gamma$ backgrounds. B_* and B_0 are respectively the branching ratios $B(D^{*+} \to D^0\pi_s^+)$ and $B(D^0 \to K^-\pi^+)$, and $\epsilon(X_E)$ is the selection efficiency as a function of X_E. The background contribution $f_{BG}(X_E)$ is determined as described in Section 3. The shape of the heavy-flavour contribution is given by

$$f_{HF}(X_E,\varepsilon_c) = \gamma_b(b/c) f_b(X_E) + \gamma_c f_c(X_E,\varepsilon_c) ,$$

where $\gamma_Q \equiv \Gamma(Z \to Q\bar{Q})/\Gamma(Z \to \text{hadrons})$. The relation $2\gamma_c + 3\gamma_b \doteq 1$ is imposed in the fit, and f_b and f_c are the expected X_E distributions from b and c contributions respectively, as obtained from the Monte Carlo, normalized to 1 for $0 \le X_E \le 1$.

Firstly, a fit with three parameters gives the following results:

$$\begin{aligned} \varepsilon_c &= (36\,^{+21}_{-14} \pm 3) \times 10^{-3} , \\ P_{c\to D^{*\pm}}\, B_*\, B_0 &= (7.0 \pm 0.6 \pm 0.7) \times 10^{-3} , \\ \gamma_c &= 0.141\,^{+0.036}_{-0.029} \pm 0.010 . \end{aligned}$$

The first errors are statistical and the second are obtained by varying the external parameters within errors. The main contribution to this uncertainty comes from the range allowed for (b/c). In this fit ε_c and γ_c are heavily correlated: the correlation coefficient is 70%.

Since γ_c is found to be consistent with the Standard Model expectation $\gamma_c^{SM} = 0.1705$, the fit is repeated with γ_c fixed to γ_c^{SM}, yielding, as a function of $\Delta = [(b/c) - 0.95]$,

$$\varepsilon_c = (47\,^{+18}_{-14}(\text{stat.}) \pm 2(\text{syst.}) - 50 \times \Delta) \times 10^{-3} ,$$

which corresponds to

$$\langle X_E(\mathrm{D}^*)\rangle_c = 0.504\,^{+0.013}_{-0.017}(\mathrm{stat.}) \pm 0.003(\mathrm{syst.}) + \Delta \times 0.05\ ,$$

and

$$P_{\mathrm{c}\to\mathrm{D}^{*\pm}}\, B_*\, B_0 = (6.7 \pm 0.4(stat.) \pm 0.3(syst.) - 3.4 \times \Delta) \times 10^{-3}\ .$$

The two fitted parameters are uncorrelated. The systematic errors come mainly from the uncertainty on the efficiency and on ε_b, and the last term is a parametrization of the 'model-dependence' of the (b/c) parameter. The latter measurement can be compared with CLEO's, performed at $\sqrt{s} = 10.55$ GeV/c. They measured the cross-section for producing a $\mathrm{D}^{*\pm}$ decaying in the mode studied here to be $17.0 \pm 1.5 \pm 1.4$ pb [11]. Dividing by the cross-section for charm production one obtains $(7.0 \pm 1.0) \times 10^{-3}$, in good agreement with the present value. In a similar way, HRS published the value 1.99 ± 0.35 for the ratio of the $\mathrm{D}^{*\pm}$ and D^{*0} production cross-section to the pointlike cross-section [14]. Translated in terms of the number of $\mathrm{D}^{*\pm}$ in the relevant decay channel per c-quark, this corresponds to $(6.6 \pm 0.5) \times 10^{-3}$, also in good agreement with the result of the study presented here.

In Fig. 4, the X_E distribution after background subtraction and correction for efficiency is shown together with the result of the fit. The two contributions, from $\mathrm{b\bar{b}}$ and $\mathrm{c\bar{c}}$, are shown separately. The χ^2 of the fit is 10.1 for 11 degrees of freedom, where the last three bins have been combined to compute the χ^2. The integral of the solid curve over the whole X_E range gives a determination of the number of $\mathrm{D}^{*\pm}$ mesons produced per hadronic decay of the Z:

$$\frac{\Gamma(\mathrm{Z} \to \mathrm{D}^{*\pm}\mathrm{X})}{\Gamma(\mathrm{Z} \to \mathrm{hadrons})}\, B_*\, B_0 = (5.11 \pm 0.34) \times 10^{-3}\ .$$

This measurement relies on the Peterson *et al.* fragmentation and the Lund parton shower model for the extrapolation to X_E values below 0.25. The results presented here are in agreement with the recent OPAL analysis [15].

The value of ε_c is obtained within the LUND model (parton shower) with $\Lambda_{\mathrm{QCD}} = 0.310$ GeV. The generated heavy-hadron energy spectra also depend on the amount of gluonic energy radiated by the primary quark before the fragmentation; ε_c thus depends on the QCD parameter Λ_{QCD}. It changes by an additional $^{+13}_{-10} \times 10^{-3}$ if the QCD scale is varied from 0.260 GeV to 0.400 GeV. The value of the average X_E, however, is almost independent of this choice.

6 Inclusive Analysis of the Decay $\mathrm{D}^{*+} \to (\mathrm{D}^0)\pi_s^+$

The search for decays of type (iii) follows the same method as in Refs. [14] and [16]. This requires only the observation of the soft pion from the decay $\mathrm{D}^{*+} \to (\mathrm{D}^0)\pi_s^+$, with a momentum in the range $1 < p < 4$ GeV/c. The cut in distance of closest approach in the transverse plane is tightened to 0.5 cm to further reject the background from decays-in-flight, and the polar angle cut is changed to $|\cos\theta| \leq 0.85$ to keep only events where the jet axis can be accurately measured.

In order to estimate the $\mathrm{D}^{*\pm}$ direction for the computation of p_{T}, charged tracks and showers from neutral particles are clustered into jets, according to the scaled-invariant-mass algorithm [17]: particles are merged together in an iterative way if their invariant mass $M_{12} = [2E_1E_2(1-\cos\theta_{12})]^{1/2}$ is less than a fixed value M_{cut}. The cluster containing the soft pion must have at least three charged tracks. Figure 5a shows the p_{T}^2 distribution for the soft tracks in six momentum bins of width 0.5 GeV/c. For this plot M_{cut} was 4.8 GeV/c^2. A clear excess of events can be seen at low p_{T}^2 when $p < 3$ GeV/c, as expected for D^* decays. The Monte Carlo simulation shows that $\langle p_{\mathrm{T}}^2\rangle = (0.08\ \mathrm{GeV}/c)^2$ and $(0.11\ \mathrm{GeV}/c)^2$ for the soft pion from the D^* decay in $\mathrm{Z} \to \mathrm{c\bar{c}}$ and $\mathrm{Z} \to \mathrm{b\bar{b}}$ events respectively, compared with the average p_{T}^2 of around $(0.3\ \mathrm{GeV}/c)^2$ from hadronization.

The fraction of D* coming from $Z \to b\bar{b}$ events depends on the π_s momentum. According to the simulation, it varies from 75% at $p = 1$ GeV/c to 9% at $p = 3$ GeV/c. For $p_T^2 < 0.01$ (GeV/c)^2 a signal-to-background ratio of about 1/9 is observed.

7 Measurement of $B_0 \equiv B(D^0 \to K^-\pi^+)$

The number of $D^{*+} \to (D^0)\pi_s^+$ decays of type (iii) has been evaluated by a fit to the observed p_T^2 distributions with two contributions:

- Background: It needs to be extrapolated into the signal region at low p_T^2. The following background parametrization has been found to provide an accurate description of the data over the range $0 < p_T^2 < (0.3$ GeV/$c)^2$:

$$F_{BG}(p_T^2) = \frac{a}{1 + bp_T^2 + c(p_T^2)^2 + d(p_T^2)^3}$$

  The fact that this simple form fits the data well over a wide p_T^2 range (Fig. 5a) lends confidence to the extrapolation to $p_T^2 = 0$. The parameters a, b, c, and d depend on the momentum bin.

- D* contributions from the $c\bar{c}$ and $b\bar{b}$ events: The approximation of the parent D* direction by the jet axis to calculate p_T^2 results in tails in the signal distribution. Therefore the p_T^2 distributions of the D*'s from $c\bar{c}$ and $b\bar{b}$ events, called $F_c(p_T^2, \varepsilon_c)$ and $F_b(p_T^2, \varepsilon_b)$, are taken from the simulation for each momentum bin, rather than using an analytical shape.

A fit to the six p_T^2 distributions of Fig. 5a is performed with the function

$$\frac{dN}{dp_T^2} = N_{had} \times 2 \times P_{c \to D^{*\pm}} B_* \, \epsilon(p) \, [\gamma_b(b/c)F_b + \gamma_c F_c] + F_{BG} \ ,$$

with the same notation as before. The efficiency $\epsilon(p)$ for selecting the soft pions varies from 85% at $p = 1$ GeV/c to 80% at $p = 3$ GeV/c. Constraining ε_c to the value derived above, one obtains

$$P_{c \to D^{*\pm}} B_* = 0.185 \pm 0.013(\text{stat.}) \pm 0.019(\text{syst.}) \pm 0.003(\text{mod. dep.})$$

with $\chi^2 = 960$ for 855 degrees of freedom. The result of the fit is also shown in Fig. 5a. The agreement in the last two momentum bins ($p > 3$ GeV/c), where the expected signal is small, demonstrates that the continuum shape is well reproduced. Figure 5b shows the p_T^2 shape of the D* signal obtained after background subtraction for all tracks with momentum between 1 and 3 GeV/c. It is compared with the expected signal of D* from $Z \to b\bar{b}$ and $Z \to c\bar{c}$ events.

The main uncertainties are now discussed:

a) The fragmentation products surrounding the D* smear the estimate of its direction as obtained from the jet axis. The Monte Carlo is relied upon to simulate this effect. The good agreement between data and Monte Carlo (Fig. 5b) illustrates the validity of this assumption. However, some inadequacies may occur in the simulation of the particle flow in the D* jet, especially from the neutrals. To obtain a conservative estimate of this effect, the jet algorithm mass cut M_{cut} has been varied from 4.8 to 17.7 GeV/c^2 and the clustering has also been restricted to the charged tracks. The relative spread (r.m.s.) in the fitted values of $P_{c \to D^{*\pm}}$, found to be ±10%, is taken as a systematic error on this parameter.

b) The p_T^2 distribution of D* from $b\bar{b}$ events is less peaked at zero than from $c\bar{c}$ events. This reduces the sensitivity of $P_{c \to D^{*\pm}}$ to the (b/c) ratio and ε_b to relative uncertainties of ±2.5% and ±1.5 % respectively.

Simultaneous measurements of the inclusive mode $D^{*+} \to (D^0)\pi_s^+$ and the exclusive mode $D^{*+} \to D^0\pi_s^+$, $D^0 \to K^-\pi^+$ allow a determination of the branching ratio of the decay $D^0 \to K^-\pi^+$:

$$B_0 \equiv B(D^0 \to K^-\pi^+) = (3.62 \pm 0.34(\text{stat.}) \pm 0.41(\text{syst.}) \pm 0.13(\text{mod.dep.}))\% \ ,$$

in good agreement with the Particle Data Group fit [10] $B_0 = (3.71 \pm 0.25)\%$ and the MARK III measurement with double-tagged D^0's [18] $(4.2 \pm 0.4 \pm 0.4)\%$.

The measurements of R_* and $P_{c \to D^{*\pm}} B_*$ can be used to determine the fraction of non-charm-strange mesons produced by primary c quarks, called f_{NCSM}. Indeed, as charmed baryons and D_s's cannot decay into $D^{*\pm}$, the following relation holds: $P_{c \to D^{*\pm}} B_* = \frac{1}{2} f_{NCSM} P_V B_* = \frac{1}{2} f_{NCSM} \frac{R_*}{1-R_*}$. The strict equality between the first and last expressions still holds in the presence of higher mass states, provided that they decay into equal proportions of charged and neutral S-wave mesons. Inserting the value of $P_{c \to D^{*\pm}} B_*$ measured in the inclusive analysis, and of R_* obtained from the exclusive decays in the $c\bar{c}$ dominated region $X_E \geq 0.5$, we determine $f_{NCSM} = 1.04 \pm 0.23$, consistent with the widely assumed value of 0.80.

8 Conclusions

Charmed meson production has been observed in ALEPH, in three different channels. The standard picture for charm production provides a very satisfactory framework to describe the data. Correcting the observed number of D^* candidates for background and efficiency leads us to the measurement:

$$\frac{\Gamma(Z \to D^{*\pm}X)}{\Gamma(Z \to \text{hadrons})} \times B(D^{*+} \to D^0\pi_s^+) \times B(D^0 \to K^-\pi^+) = (5.11 \pm 0.34) \times 10^{-3} \ .$$

The relative production rate of vector and pseudoscalar charmed mesons has also been measured. For a mixture of equal proportions of D^*'s from $Z \to c\bar{c}$ and $Z \to b\bar{b}$ decays, and if the presence of higher mass states can be neglected, the $V/(V+P)$ ratio is

$$P_V = (0.60 \pm 0.08) \times \frac{0.55}{B(D^{*+} \to D^0\pi_s^+)} \ .$$

From a fit to the D^* energy spectrum , the following two parameters have been determined:

- the average fractional energy carried by the D^* meson:
  $\langle X_E \rangle_c = 0.504\,^{+0.013}_{-0.017}(\text{stat.}) \pm 0.008(\text{syst.})$
- the probability for producing a $D^{*\pm}$ subsequently decaying into $K\pi\pi$:
  $P_{c \to D^{*\pm}} \times B(D^{*+} \to D^0\pi_s^+) \times B(D^0 \to K^-\pi^+) = (6.7 \pm 0.4(\text{stat.}) \pm 0.7(\text{syst.})) \times 10^{-3}$

In all the results given in this section, the systematic error takes into account the dependence on the choice of (b/c).

The simultaneous observation of the different signals leads to the measurements:

$$P_{c \to D^{*\pm}} \times B(D^{*+} \to D^0\pi_s^+) = 0.185 \pm 0.013(\text{stat.}) \pm 0.020(\text{syst.})$$

and

$$B(D^0 \to K^-\pi^+) = (3.62 \pm 0.34(\text{stat.}) \pm 0.44(\text{syst.}))\% \ .$$

Acknowledgements

We wish to congratulate our colleagues in the CERN accelerator division for operating the LEP storage ring. We are grateful to the engineers and technicians in all our institutions for their contribution towards ALEPH's success. We thank T. Sjöstrand for useful discussions. Those of us from non-member countries thank CERN for its hospitality.

References

[1] S. Nussinov, Phys. Rev. **D35** (1975) 1672.

[2] D. Decamp *et al.* (ALEPH Collab.), Nucl. Instrum. Methods A **294** (1990) 121.

[3] W. Atwood *et al.*, 'Performance of the ALEPH Time Projection Chamber', submitted to Nucl. Instrum. Methods A.

[4] D. Decamp *et al.* (ALEPH Collab.), 'Improved Measurements of Electroweak Parameters from Z decay into Fermion Pairs', preprint CERN-PPE/91-105 (1991), submitted to Z. Phys. C.

[5] T.Sjöstrand and M. Bengtsson, Comput. Phys. Commun. **46** (1987) 43.

[6] C. Peterson, D. Schlatter, I. Schmitt and P. M. Zerwas, Phys. Rev. **D 27** (1983) 105.

[7] D. Decamp *et al.* (ALEPH Collab.), Phys. Lett. **B 244** (1990) 551.

[8] H. Albrecht *et al.* (ARGUS Collab.), Phys. Lett. **B 150** (1985) 235.

[9] S. Abachi *et al.* (HRS Collab.), Phys. Lett. **B 212** (1988) 533.

[10] Particle Data Group, Phys. Lett. **B 239** (1990).

[11] D. Bortoletto *et al.* (CLEO Collab.), Phys. Rev. **D 37** (1988) 1719; Phys. Rev. **D 39** (1989) 1471.

[12] R. Kass, 'Charm Particle Decay', Talk given at the 4th International Symposium on Heavy Flavour Physics, 25-29 June 1991, Orsay, France.

[13] H. Albrecht *et al.* (ARGUS Collab.), Phys. Rev. Lett. **56** (1986) 549; H. Albrecht *et al.* (ARGUS Collab.), Phys. Lett. **B 221** (1989) 422; H. Albrecht *et al.* (ARGUS Collab.), Phys. Lett. **B 231** (1989) 208; P. Avery *et al.* (CLEO Collab.), Phys. Rev. **D 41** (1990) 774; R. Fulton *et al.* (CLEO Collab.), Phys. Rev. **D 43** (1991) 651.

[14] S. Abachi *et al.* (HRS Collab.), Phys. Lett. **B 205** (1988) 411; P. Baringer *et al.* (HRS Collab.), Phys. Lett. **B 206** (1988) 551.

[15] G. Alexander et al. (OPAL Collab.), 'A Study of $D^{*\pm}$-Production in Z^0 Decays', preprint CERN-PPE/91-63 (1991).

[16] P. Abreu *et al.* (DELPHI Collab.), Phys. Lett. **B 252** (1990) 140.

[17] W. Bartel *et al.* (JADE Collab.), Z. Phys. **C 33** (1986) 23.

[18] J. Adler *et al.* (MARK III Collab.), Phys. Rev. Lett. **60** (1988) 89.

Figure captions

Fig. 1. Kπ invariant mass distribution, for $X_E(\mathrm{K}\pi) > 0.25$. Data (points with error bars) compared with the fit described in the text.

Fig. 2. Mass-difference distribution, for $X_E(\mathrm{K}\pi\pi) > 0.25$. The K$\pi$ mass is required to be between 1.835 and 1.895 GeV/c^2. a) The background, calculated by the event-mixing technique, is shown. The curve is a fit to the data with a power law for the background and the sum of two Gaussians for the signal. b) Comparison of the data with the Monte Carlo (histogram).

Fig. 3. Kπ invariant mass distribution, for D* candidates with $X_E(\mathrm{K}\pi\pi) > 0.25$. The mass difference ΔM is required to be between 0.1435 and 0.1475 GeV/c^2. Data (points with error bars) compared with the fit described in the text (the event-mixing technique is used for the combinatorial background). The second peak around 1.6 GeV/c^2 is due to D $\rightarrow$ KπX.

Fig. 4. $X_E(\mathrm{D}^*)$ distribution, corrected for efficiency and background subtracted. The data are represented by dots with error bars; the best fit is shown (solid line), together with $\mathrm{b\bar{b}}$ and $\mathrm{c\bar{c}}$ contributions.

Fig. 5. a) p_{T}^2 of hadrons in six momentum bins, 0.5 GeV/c wide. The momentum, between 1 and 4 GeV/c, increases from top to bottom. The D* signal, in the low-p and low-p_{T}^2 region, is clearly visible. b) Detail of the low-p_{T}^2 region, background subtracted, for $1 < p < 3$ GeV/c. The fitted $\mathrm{b\bar{b}}$ and $\mathrm{c\bar{c}}$ contributions are shown. The p_{T}^2 shape of the signal is well modelled by the simulation.

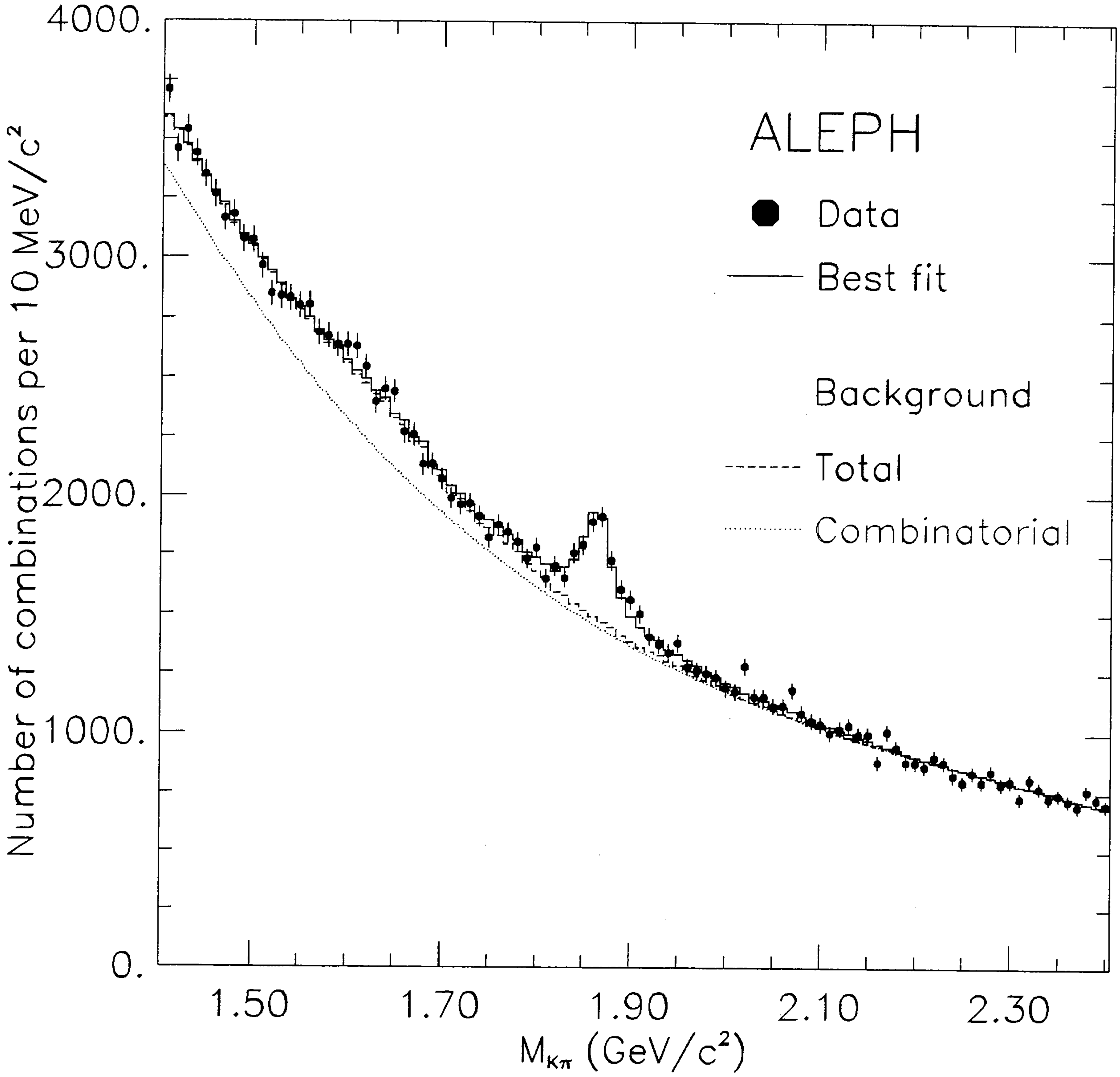
ALEPH
Data
Best fit
Background
Total
Combinatorial
Number of combinations per 10 MeV/c²
M$_{K\pi}$ (GeV/c²)
4000.
3000.
2000.
1000.
0.
1.50
1.70
1.90
2.10
2.30

Fig. 1

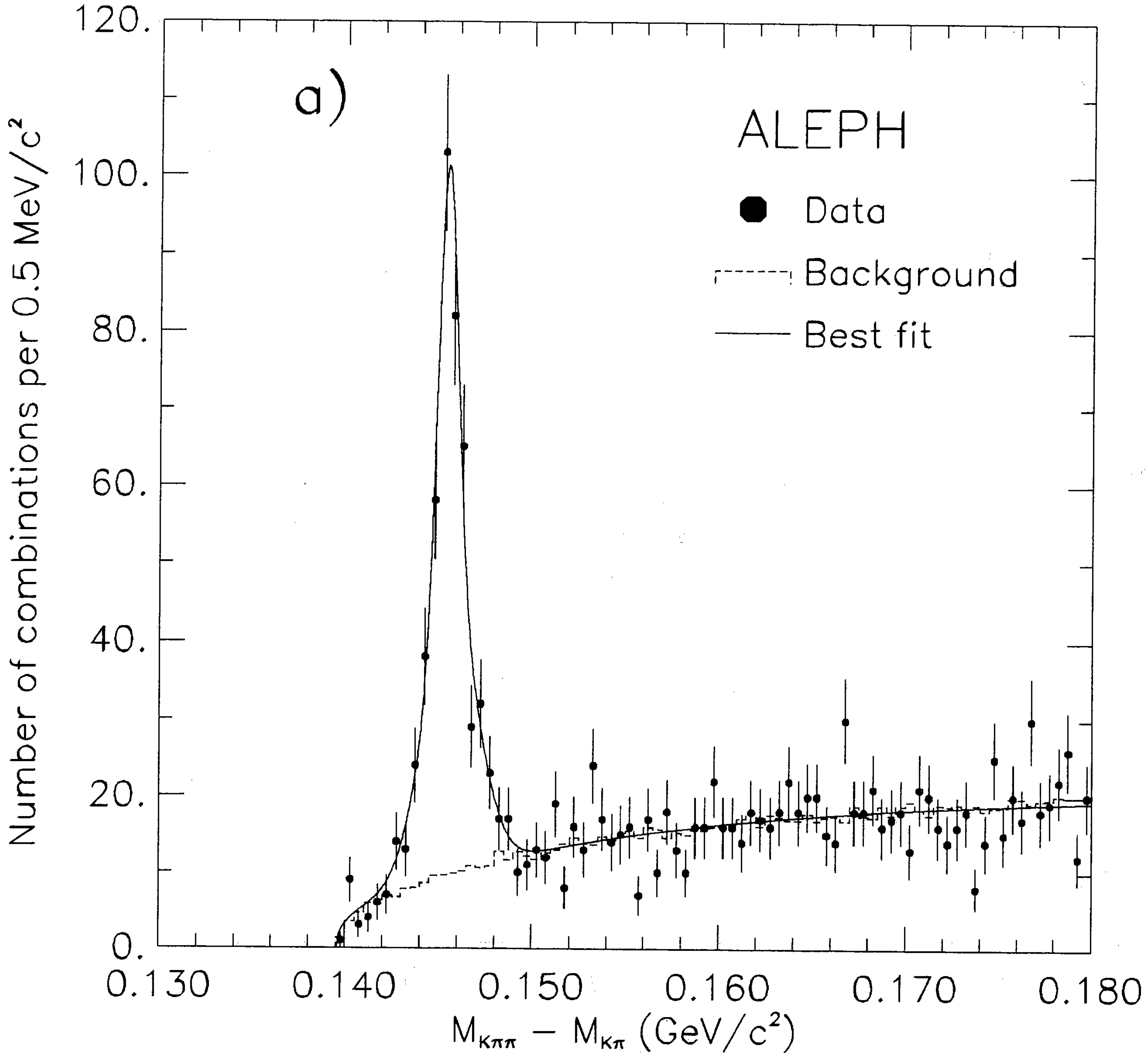

a)
ALEPH
Data
Background
Best fit
Number of combinations per 0.5 MeV/c²
M_{Kππ} − M_{Kπ} (GeV/c²)
120.
100.
80.
60.
40.
20.
0.
0.130
0.140
0.150
0.160
0.170
0.180

Fig. 2a

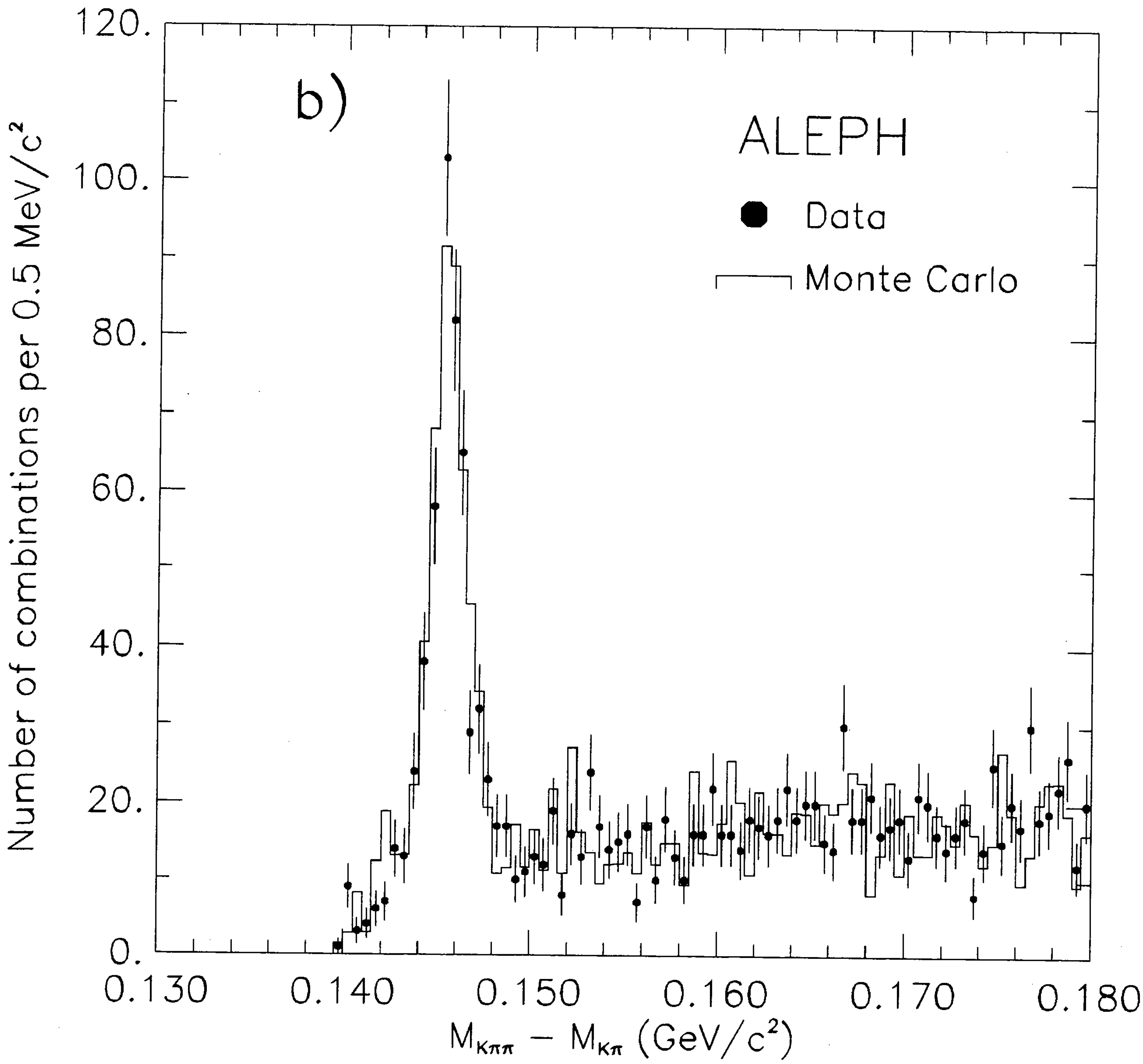

120.
100.
80.
60.
40.
20.
0.
b)
ALEPH
Data
Monte Carlo
Number of combinations per 0.5 MeV/c²
0.130
0.140
0.150
0.160
0.170
0.180
M_Kππ − M_Kπ (GeV/c²)

Fig. 2b

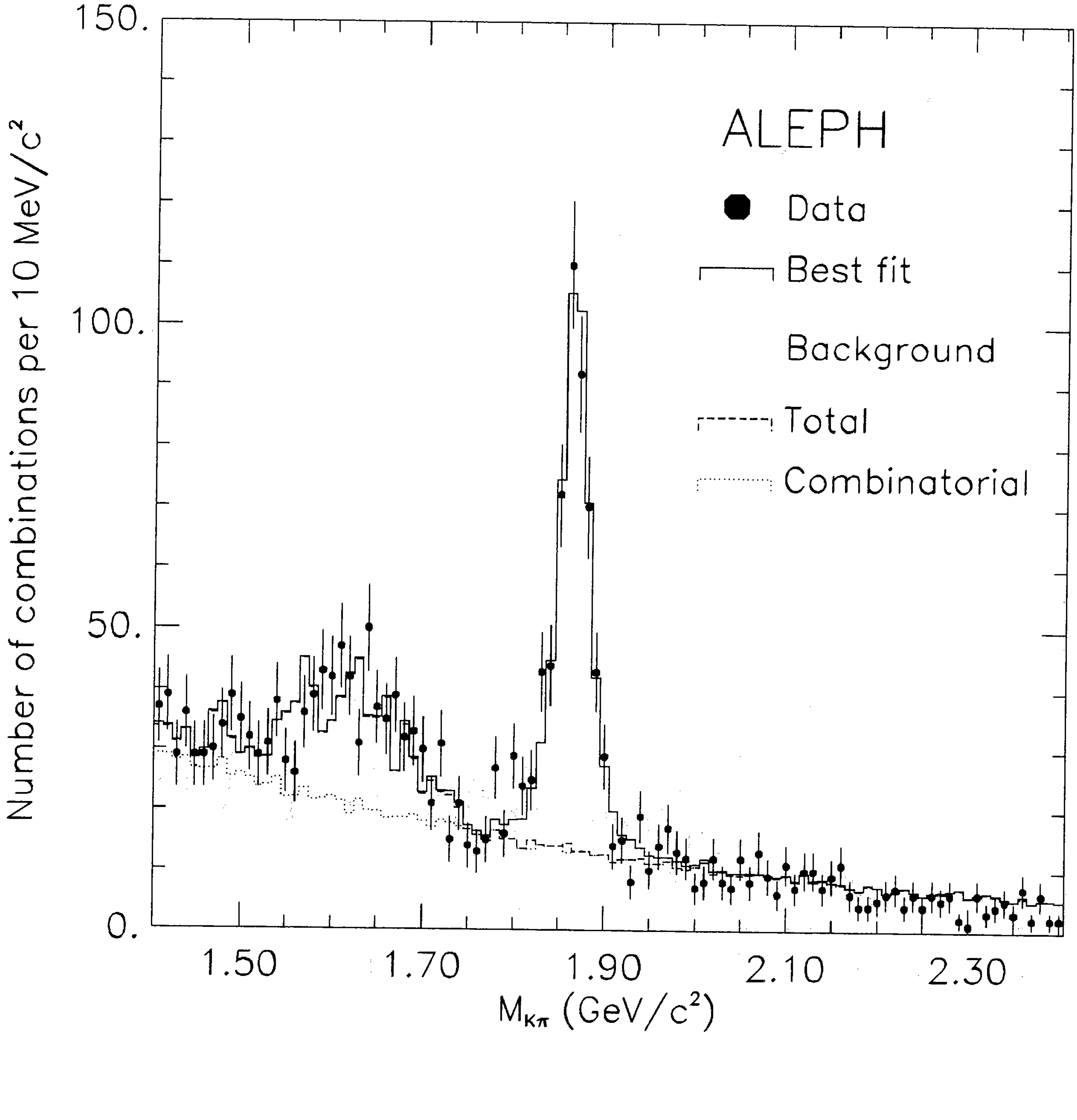

ALEPH
Data
Best fit
Background
Total
Combinatorial
Number of combinations per 10 MeV/c²
150.
100.
50.
0.
1.50
1.70
1.90
2.10
2.30
M_Kπ (GeV/c²)

Fig. 3

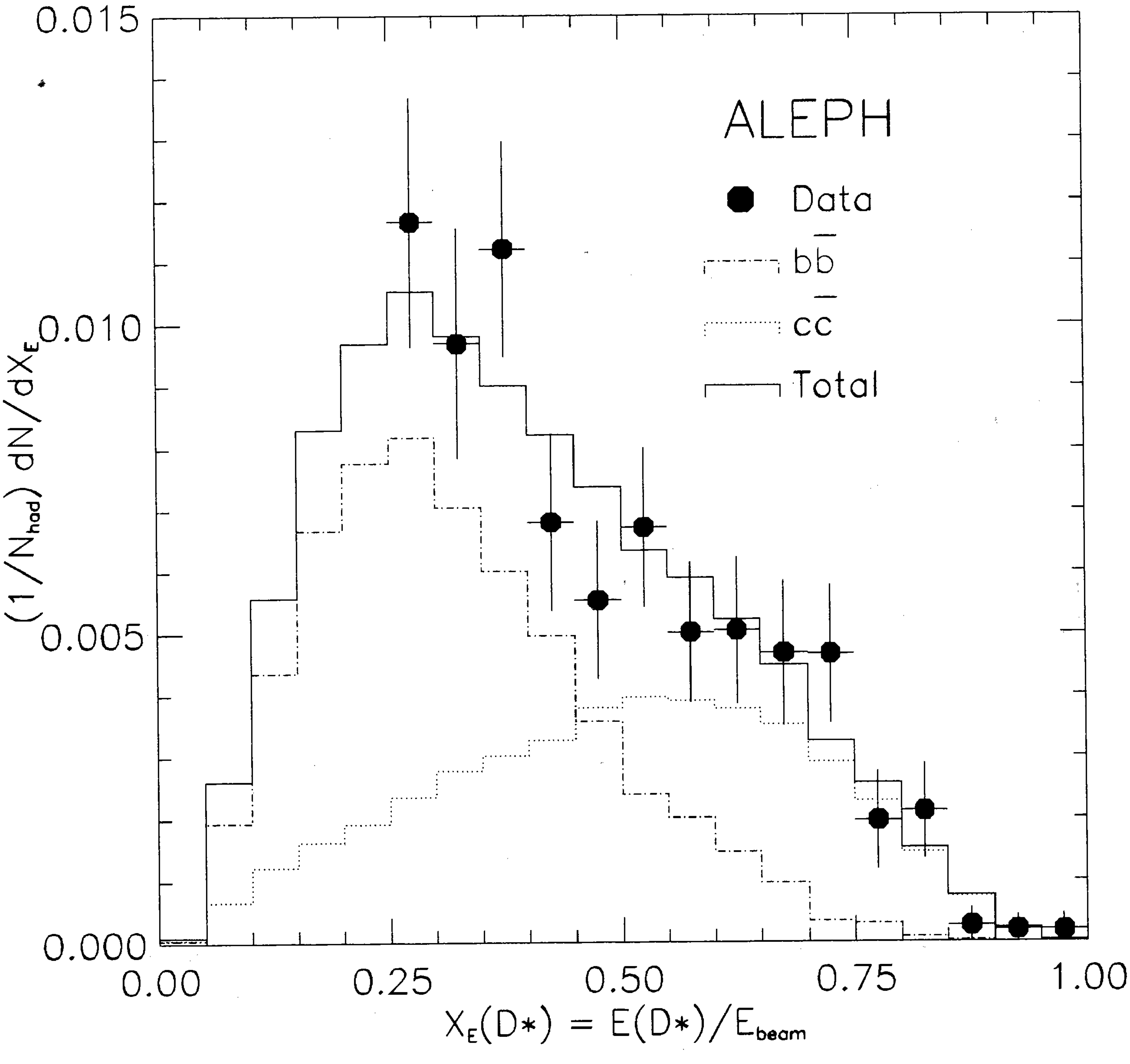

ALEPH
Data
$b\bar{b}$
$c\bar{c}$
Total
0.015
0.010
0.005
0.000
$(1/N_{had})\ dN/dX_E$
0.00
0.25
0.50
0.75
1.00
$X_E(D*) = E(D*)/E_{beam}$

Fig. 4

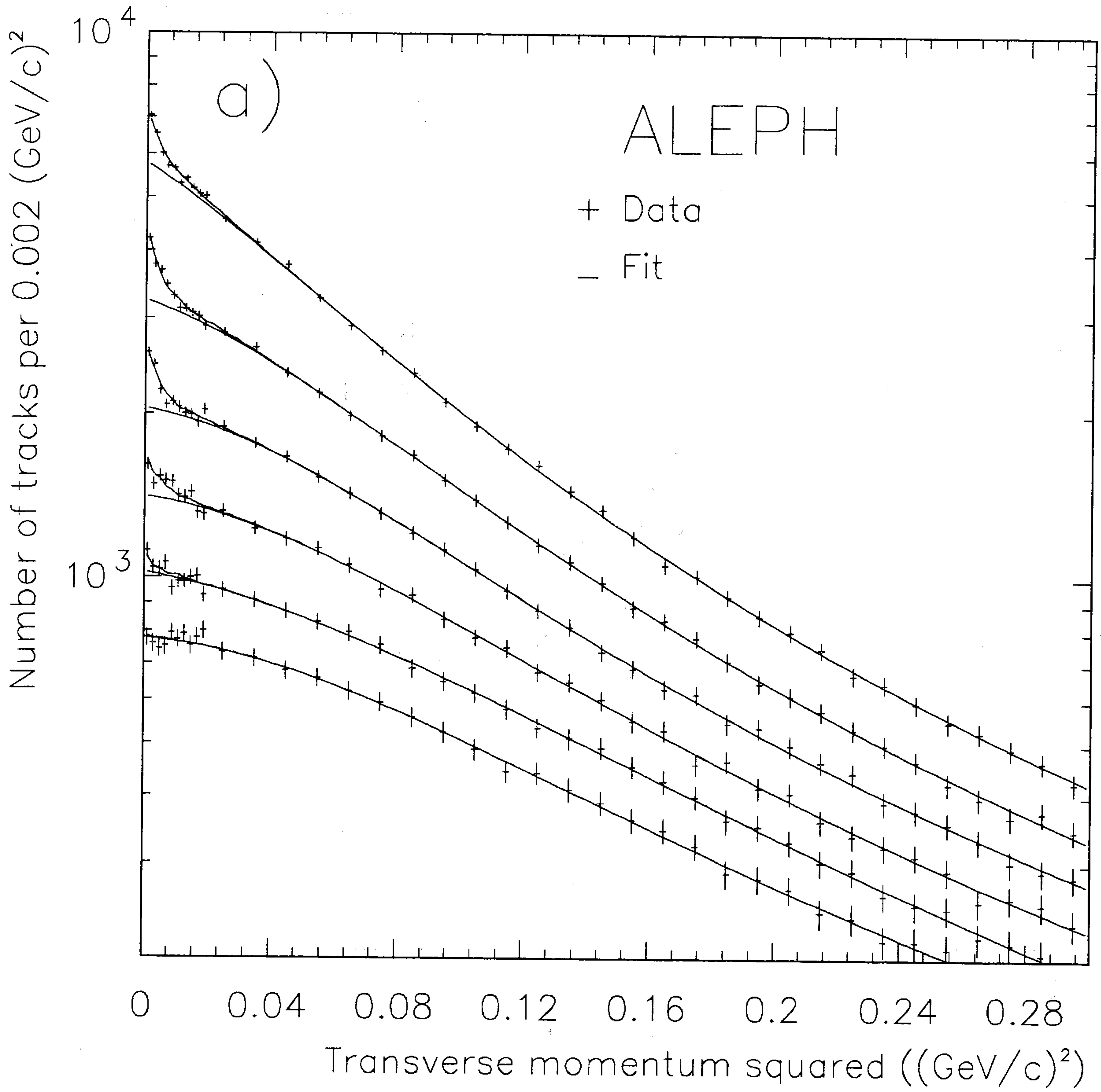
a)
ALEPH
+ Data
_ Fit
Number of tracks per 0.002 (GeV/c)²
Transverse momentum squared ((GeV/c)²)
10⁴
10³
0
0.04
0.08
0.12
0.16
0.2
0.24
0.28

Fig. 5a

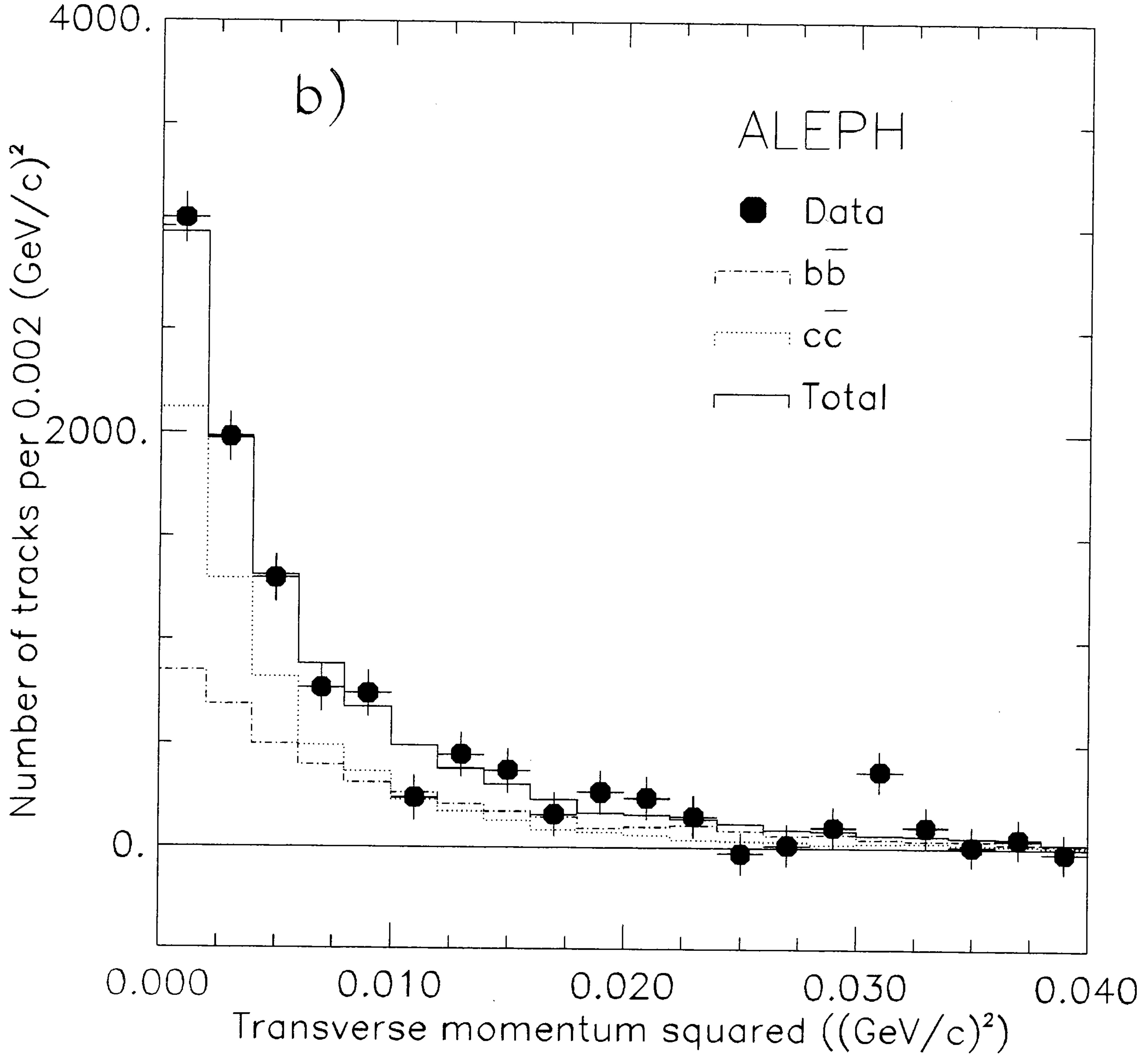

b)
ALEPH
Data
$b\bar{b}$
$c\bar{c}$
Total
4000.
2000.
0.
0.000
0.010
0.020
0.030
0.040
Number of tracks per 0.002 (GeV/c)²
Transverse momentum squared ((GeV/c)²)

Fig. 5b